

Article

Preparation of PAN@TiO₂ Nanofibers for Fruit Packaging Materials with Efficient Photocatalytic Degradation of Ethylene

Zhu Zhu ¹, Ye Zhang ², Yibo Zhang ², Yanli Shang ^{2,*}, Xueji Zhang ¹ and Yongqiang Wen ^{1,*}

¹ Beijing Key Laboratory of Bioengineering and Sensing Technology, School of Chemistry and Bioengineering, University of Science & Technology Beijing, Beijing 100083, China; zhuzhu@ustb.edu.cn (Z.Z.); zhangxueji@ustb.edu.cn (X.Z.)

² College of Chemistry & Environmental Science, Hebei University, Baoding 071002, China; 18330117319@163.com (Y.Z.); ybzhang0123@163.com (Y.Z.)

* Correspondence: shyl@iccas.ac.cn (Y.S.); wyq_wen@iccas.ac.cn (Y.W.); Tel.: +86-312-5077393 (Y.S.); +86-10-82375840 (Y.W.)

Received: 14 February 2019; Accepted: 13 March 2019; Published: 18 March 2019



Abstract: Ethylene causes faster deterioration of perishable crops during postharvest transportation and storage. The present study aimed to develop TiO₂-coated nanofibers with efficient photocatalytic activities to enhance the degradation of fruit-emitted ethylene. The consecutive electrospinning of polyacrylonitrile (PAN) and TiO₂ deposition was successfully performed to produce PAN@TiO₂ nanofibers. The scanning electron microscopy results indicate the uniform distribution of TiO₂ nanoparticles on the surface of the PAN nanofiber. The PAN@TiO₂ composite nanofibers exhibited enhanced photocatalytic activity for ethylene degradation under low-intensity UV light irradiation. Furthermore, a tomato fruit-ripening test confirmed the effectiveness of the PAN@TiO₂ nanofibers. The PAN@TiO₂ nanofibers exhibited effective ethylene degradation and slowed the color shift and softening of the tomatoes during storage. The results suggest great potential for use of the PAN@TiO₂ composite nanofibers as ethylene scavenging packaging material for fresh fruits and vegetables.

Keywords: electrospun nanofiber; TiO₂; photocatalytic activity; ethylene degradation; tomato ripening

1. Introduction

Ethylene is a natural aging hormone that enhances the decay of perishable crops during postharvest transportation and storage. Hence, removing ethylene from the environment surrounding fresh produce plays a pivotal role in prolonging their shelf life and reducing postharvest losses [1]. Currently, active packaging, which involves the addition of active component in packaging systems, is widely implemented to maintain or extend food product qualities and shelf lives [2]. Several ethylene scavenging packaging systems have been developed for fruits and vegetables. Potassium permanganate (KMnO₄) or activated carbon is used in the form of sachets [3,4]; and clays and halloysite nanotubes are incorporated into films as ethylene scavenging materials [5,6]. However, these oxidizers and absorbers are limited by waste disposal and limited adsorption capacity [7]. Emerging technologies based on photocatalytic oxidation of ethylene offer an alternative approach that could overcome these disadvantages.

The photocatalytic oxidation of ethylene involves exposure to ultra violet (UV) radiation and the use of a catalyst such as titanium dioxide (TiO₂). In general, reactive oxygen species (ROS) are produced on the TiO₂ surface following exposure to UV light, thereby further oxidizing ethylene to carbon dioxide and water [8]. In the past decade, several composite films containing TiO₂ to remove ethylene at different UV light intensity ranging from 42 μW cm⁻² to 2.5 mW cm⁻² have been reported.

Tanaka et al. [9] prepared an adsorbents-embedded TiO₂ film by sol-gel method. Maneerat and Hayata [10] used a polypropylene film coated with TiO₂ as an ethylene scavenger packaging material. A chitosan–TiO₂ nanocomposite film was also fabricated to prolong shelf life of tomato fruit [11].

Nanofibers offer some advantages over ordinary films including high surface-to-volume ratio, nanoporous structures and easy encapsulation of active agents [12]. Electrospinning provides a quick approach to fabricating continuous nanofibers and has been used to prepare inorganic nanoparticles in polymers. In our previous study, TiO₂-embedded nanofibers were prepared by adding TiO₂ nanoparticles into the polymer solution via one step electrospinning [13]. However, the homogeneous dispersion of nanoparticles in a polymer matrix is challenging due to the resulting agglomeration of nanoparticles and the high viscosity of polymers. Furthermore, the presence of a polymer layer surrounding the nanoparticles limits the interaction between the particle surface and oxygen or water.

To address these problems, researchers have deposited inorganic nanoparticles on the surface of the nanofiber. For example, Hong et al. [14] fabricated PVA/ZnO composites via electrospinning followed by an in situ hydrolysis process; the ZnO nanocrystals were formed on the fiber surface with high density. Gupta et al. [15] achieved TiO₂ deposition onto polylactic acid (PLA) nanofibers via hydrothermal synthesis and electrospinning, of which the resulting PLA/TiO₂ nanofibers exhibited excellent UV absorption properties.

The present study consecutively performed polyacrylonitrile (PAN) electrospinning followed by TiO₂ deposition to produce PAN@TiO₂ composite nanofibers, of which the TiO₂ nanoparticles were assembled on the surface of the fiber rather than within the nanofibers to enhance its photocatalytic activity for the degradation of fruit-emitted ethylene. The morphology and the crystallinity of the produced composite nanofibers were investigated. The photocatalytic activity of the composite nanofibers in the degradation of ethylene was determined. The results show that the surface of the composite was coated with a larger amount of TiO₂ nanoparticles, which could effectively increase the contact area between nanoparticles and ethylene and improve the degradation efficiency of ethylene. The composite nanofibers were then used to retard tomato fruit ripening during postharvest storage.

2. Materials and Methods

2.1. Materials

Ammonium sulfate ((NH₄)₂SO₄), titanium tetrachloride (TiCl₄), dimethylformamide (DMF), and ammonia (NH₃·H₂O) were purchased from Beijing Chemicals (Beijing, China). PAN (polyacrylonitrile, M_w = 150,000) was obtained from Aladdin Reagent (Shanghai, China). Ethylene (99.995%) was obtained from Beijing ZG Gas Science & Technology Co., Ltd (Beijing, China). The tomatoes were harvested at the mature green stage from a greenhouse and sorted according to color and size without physical injuries or decay. All of the chemicals were of analytical reagent grade.

2.2. Fabrication of PAN Nanofibers

PAN was dissolved in DMF to produce a polymer solution that was then loaded into a syringe equipped with a stainless-steel needle. The samples were collected using an aluminum sheet at a distance of 17 cm from tip to collector. The polymer solution was pumped at a constant rate of 0.5 mL/h, and at a voltage of 24 kV. The nanofibers were then dried overnight in a vacuum oven to allow solvent evaporation.

2.3. TiO₂ Deposition on Nanofibers

The PAN@TiO₂ nanofibers were prepared following the methodology described by Shi et al. [16]. In an ice-water bath, 2.7 mL of TiCl₄ was slowly added into a flask containing 45 mL of a (NH₄)₂SO₄ solution (1 M) under vigorous stirring. The solution was then slowly heated to 90 °C, and a 0.2 g PAN nanofiber was immersed in this solution. The mixture was reacted at 90 °C for 1 h, and the pH of the solution was then adjusted to 7 via the addition of 2 M NH₃·H₂O. The solution mixture was cooled to

room temperature, after which the nanofiber was removed, and washed three times with deionized water and vacuum-dried overnight at 30 °C.

2.4. Characterization of the Nanofiber

The PAN and PAN@TiO₂ microstructures were characterized via scanning electron microscopy (SEM, SUPRA55, ZEISS, Berlin, Germany) and transmission electron microscopy (TEM, HT7700, Hitachi, Tokyo, Japan). The elemental composition of the nanofibers was confirmed by energy dispersive X-ray spectroscopy (EDS, XFlash 5010, Bruker, Berlin, Germany). The crystalline structure of the PAN@TiO₂ nanofibers was examined with X-ray diffraction (XRD, D8 ADVANCE, Bruker, Berlin, Germany) using Cu K α radiation ($\lambda = 1.540 \text{ \AA}$). The infrared spectra of the PAN and PAN@TiO₂ nanofibers were recorded using a Fourier transform infrared spectrometer (FTIR, Nicolet Nexus 670) (Thermo Nicolet Corporation, Nikolai, America) in the range from 500 cm⁻¹ to 4000 cm⁻¹. UV-vis diffuse reflectance spectra of nanofiber were recorded on a UV-Vis spectrophotometer (TU-1901, Purkinje General, Beijing, China). The nanofiber samples were mixed with BaSO₄ and compressed into a tablet. BaSO₄ was used as a reflectance standard.

2.5. Photocatalytic Degradation of Ethylene

Ethylene degradation was carried out in a 5.4-L reactor under a UV lamp (16 W) (Haimen Kylin-Bell Lab Instruments Co., Ltd., Nantong, China), which had an intensity of 2.9 $\mu\text{W cm}^{-2}$. The nanofibers were attached to the inner surface, and rubber plugs were used to plug the inlet and outlet.

One hundred parts per million of ethylene was then injected into the reactor, and the gaseous mixture was homogenized with a fan. After achieving steady-state conditions, the initial concentration of ethylene was measured with a handheld ethylene analyzer (F-950, CID Bio Science Inc. Shanghai, China) that automatically collected headspace samples. Then, the UV light was turned on, and the ethylene concentration was measured every 5 h. The ethylene degradation C (%) was calculated as follows:

$$C = \frac{(C_i - C_f)}{C_i} \times 100\%$$

where C_i and C_f are the initial and final concentrations of ethylene, respectively. The results were expressed as a percentage of ethylene degradation.

2.6. Fruit Ripening Test

Tomatoes were randomly distributed into two groups and placed in plastic boxes that are open at the top, specifically three boxes per group and eight fruits per box. Tomatoes were identical in each box. The boxes of the first group were fully covered with a layer of polypropylene (PP) film (25 μm thick, 72% transmittance at a wavelength of 365 nm) and served as the control. The boxes of the second group were fully covered with a layer of PAN@TiO₂ nanofiber and a layer of PP film. The UV lamp was suspended above the boxes, the intensity was measured using a radiation meter, and was adjusted to 2.9 $\mu\text{W cm}^{-2}$ by adjusting the distance between the light and the boxes. All of the boxes were stored at room temperature (22 °C) under UV irradiation until the fruits in the control groups were fully ripe. To determine the ethylene production, four fruit from each box were sealed in a gas-tight container for 3 h, and the concentration was measured as described above. The fruit firmness was measured with a digital fruit firmness tester (GY-4, Zhejiang Top Instrument Co., Ltd. Hangzhou, China) that was fitted with a cylindrical plunger (diameter, 3.5 mm). Each assay had three replicates, and the experiment was performed in triplicate.

3. Results and Discussion

3.1. Characteristics of the PAN@TiO₂ Nanofibers

PAN is the widely used polymer matrix due to its high mechanical properties and chemical inertness [17]. The PAN nanofibers had smooth surfaces and nanometer-scale diameters (Figure 1A).

TiCl_4 served as the Ti precursor and the addition of SO_4^{2-} promoted the formation of anatase TiO_2 . TiCl_4 followed a three-step hydrolysis mechanism, and the TiO_2 precipitate was collected after temperature increased to $95\text{ }^\circ\text{C}$ [18]. The TiO_2 precipitate was positively charged due to the lower pH level of the mixed solution ($\text{pH} < 1$) [19]. Therefore, TiO_2 with positive charges was attracted by the nitrile group of PAN with electronegativity to form nucleation sites. Enhanced TiO_2 growth was observed on the nucleation sites following the addition of dilute $\text{NH}_3\cdot\text{H}_2\text{O}$. The morphology of the PAN@ TiO_2 nanofibers is detailed in Figure 1B,C. The TiO_2 nanoparticles were immobilized on the surface of the PAN nanofiber. The images demonstrate that the PAN nanofibers were successfully decorated with TiO_2 . The elemental composition of PAN@ TiO_2 nanofibers was confirmed by EDS mapping analysis. The images show that the sample contained C, O, and Ti elements, and the Ti element was well dispersed throughout the nanofiber (Figure 1D–F).

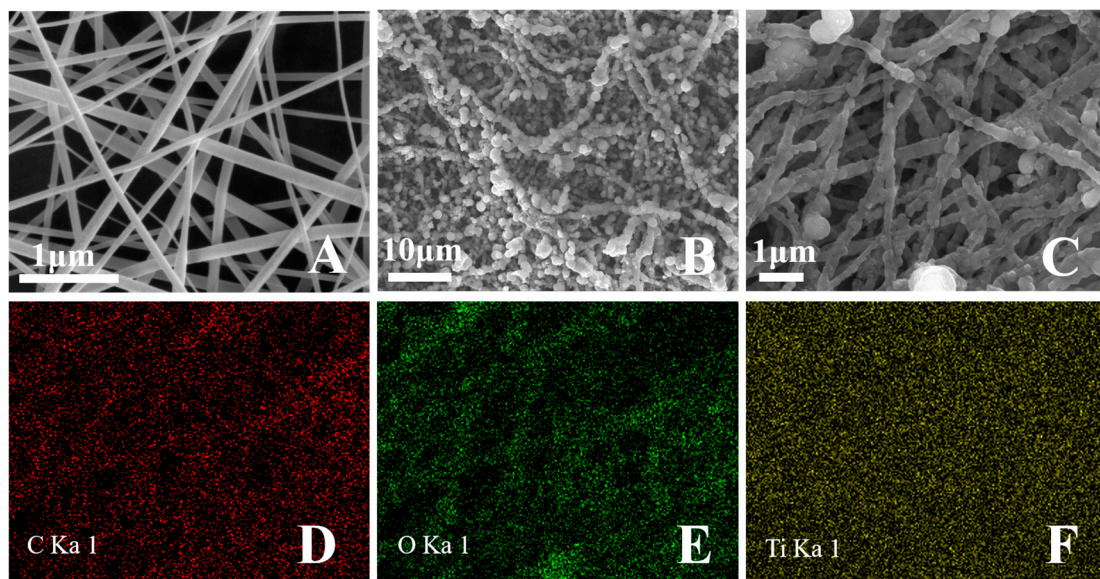


Figure 1. Scanning electron microscopy (SEM) images of: (A) electrospun PAN nanofibers; (B) PAN@ TiO_2 nanofibers at low magnification; and (C) PAN@ TiO_2 nanofibers at high magnification. EDS mapping images of PAN@ TiO_2 nanofibers: (D) carbon; (E) oxygen; and (F) titanium.

The microstructures of the nanoparticle-modified nanofiber were further characterized by TEM. Figure 2B presents the uniform distribution of the TiO_2 nanoparticles along the nanofibers. This confirmed the continuous coating of TiO_2 on the PAN nanofiber.

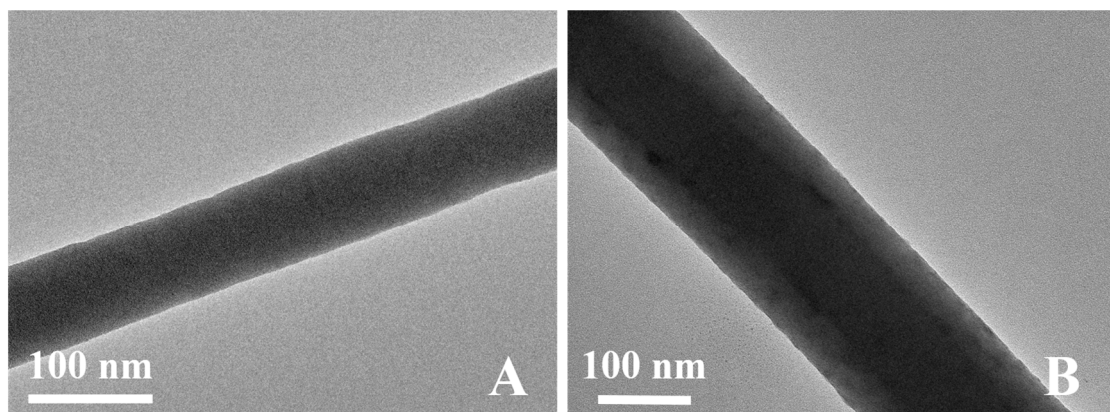


Figure 2. Transmission electron microscopy (TEM) images of: (A) electrospun PAN nanofibers; and (B) PAN@ TiO_2 nanofibers.

The crystalline structure of the synthesized TiO_2 was examined by XRD (Figure 3), in which a peak at 17° was observed, indicating the presence of PAN [20]. Other diffraction peaks were well indexed to anatase TiO_2 , suggesting that the synthesized TiO_2 nanoparticles on the nanofibers were in the anatase phase. The crystal phase may have affected the photocatalytic efficiency, given that the anatase phase manifests a higher photocatalytic activity compared to the rutile and brookite phases [21]. For crystalline structure control, SO_4^{2-} was bridged by Ti^{4+} to help form anatase phase TiO_2 ; otherwise, TiO_2 had both rutile and anatase phase [18]. Moreover, the average crystallite size of TiO_2 was calculated by the Scherrer equation: $D = 0.89 \lambda / (\beta \cos \theta)$, where λ is the X-ray wavelength, $\lambda = 0.154056 \text{ nm}$, θ is the Bragg's diffraction angle, and β is the full width at half maximum. When β is 0.015 rad and θ is 12.67° , the crystallite size of TiO_2 is 9.1 nm. It has been demonstrated that the nanoparticles in the range of 1–10 nm exhibit excellent catalytic characters owing to the quantum size effect [22,23].

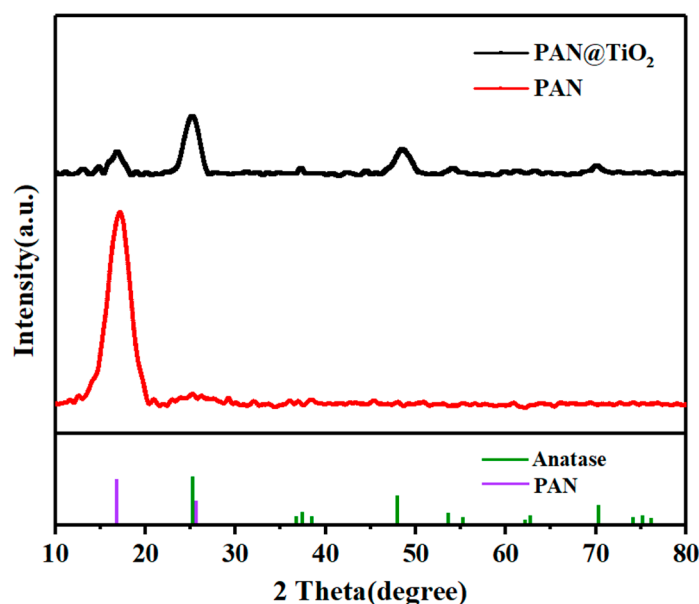


Figure 3. X-ray diffraction (XRD) patterns of PAN and PAN@ TiO_2 nanofibers.

The FTIR spectra of the PAN and PAN@ TiO_2 nanofibers were analyzed to examine the conversion of precursor chemical structure of the polymers (Figure 4). The FTIR spectra of the PAN nanofibers presented characteristic peaks at 2928, 2240, 1738, 1454, 1240 and 1033 cm^{-1} , corresponding to CH stretching, $\text{C}\equiv\text{N}$ stretching, $\text{C}=\text{O}$ stretching, CH bending, CH rocking vibrations, and $\text{C}=\text{O}$ rocking vibrations. After coating with TiO_2 , the spectrum of nanofibers showed distinct changes. Observed peaks ranging from 750 to 900 cm^{-1} corresponded to Ti-O stretching vibration. Similarly, an absorption peak observed at 3200 cm^{-1} suggested OH stretching vibration. Some water molecules in the air may have been adsorbed onto the surface of TiO_2 , such that the absorbance peak of hydroxyl can be attributed to the presence of Ti-OH on the surface of TiO_2 [24]. These results demonstrate that TiO_2 were successfully deposited onto PAN nanofibers, and the structure of TiO_2 was not changed.

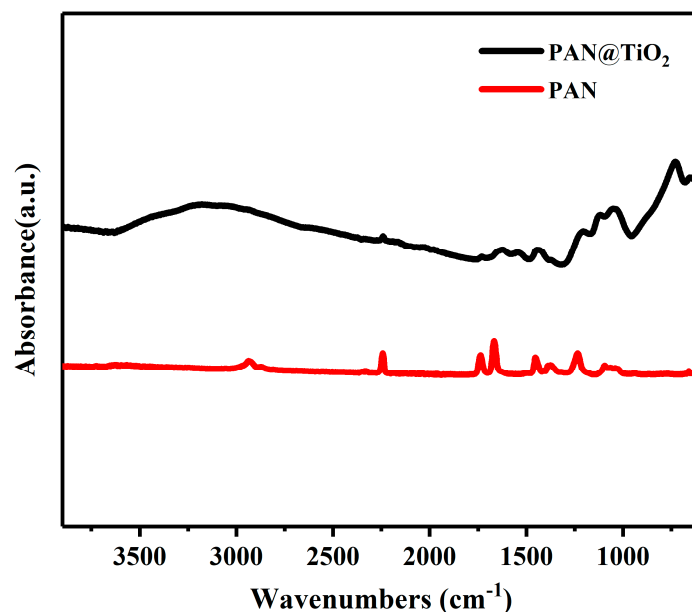


Figure 4. Fourier transform infrared spectrometer (FTIR) spectra of PAN and PAN@TiO₂ nanofibers in the range of 4000 cm⁻¹ to 500 cm⁻¹.

UV absorption spectra of PAN and TiO₂-coated nanofibers were recorded to evaluate their photoactive nature (Figure 5). Pure PAN nanofibers exhibited no absorption in UV region, while the TiO₂-coated nanofibers had great absorption in the range of UV spectrum. The result are consistent with a previous study showing that TiO₂ nanotubes absorbed UV light in the 300–400 nm range [25].

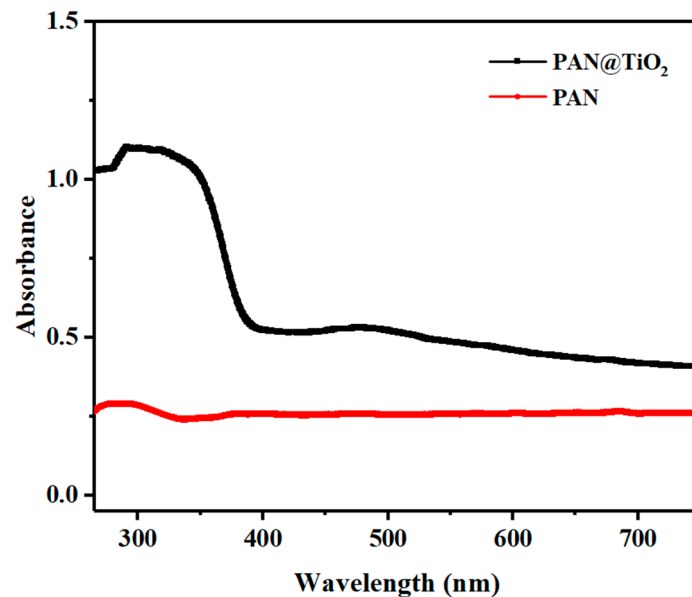


Figure 5. UV-vis diffuse reflectance spectra of PAN and PAN@TiO₂ nanofibers.

3.2. Photocatalytic Degradation of Ethylene

The ethylene degradation efficiency of the PAN@TiO₂ nanofibers were measured under UV illumination to evaluate their photocatalytic behavior. Under UV light, electrons on the TiO₂ surface are promoted and transferred from valence band to the conduction band, leaving behind holes in the valence band. These electron-hole pairs are highly charged and can initiate reduction and oxidation reaction. In the presence of air and water, hydroxyl radicals and superoxide ions are generated to oxidize ethylene into carbon dioxide and water [8]. As indicated in Figure 6, ethylene degradation of

PAN@TiO₂ nanofibers was positively correlated with the UV irradiation time. Approximately 65% of the ethylene was degraded within 25 h. In contrast, ethylene content decreased slightly for pure PAN nanofibers, which was probably because the nanofibers with nanoporous structures and large surface area adsorbed a small amount of ethylene. The results demonstrate that TiO₂-coated PAN nanofibers showed much higher photocatalytic activity than the TiO₂-embedded nanofibers [13]. The well-separated TiO₂ on the surface of the PAN nanofibers could be easily accessible to oxygen, water, and ethylene surrounding the nanoparticles. Furthermore, the homogeneous distribution throughout the nanofiber could enhance the contact area with UV light to remove ethylene [26].

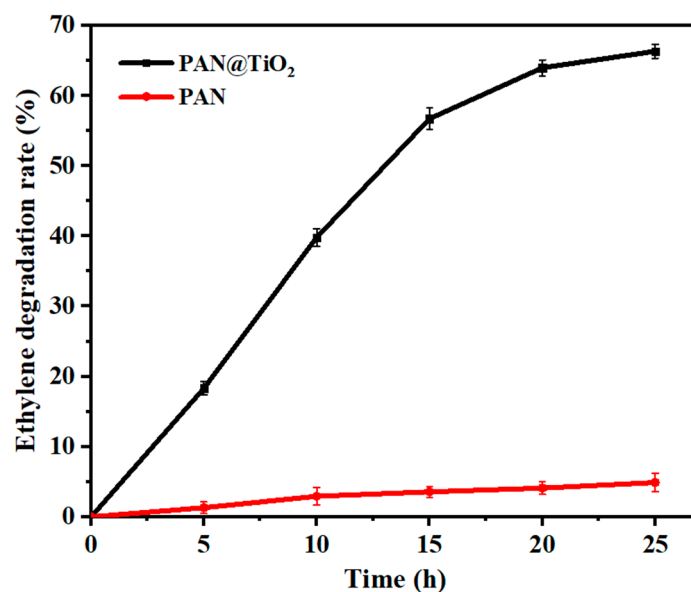


Figure 6. Photocatalytic degradation of ethylene using PAN@TiO₂ nanofibers under UV irradiation. The data represent the means of three independent experiments. The error bars indicate the standard deviation of the mean.

3.3. Tomato Ripening Test

The photocatalytic activity of the PAN@TiO₂ nanofibers were further evaluated using a tomato fruit-ripening test, wherein the significant increase in ethylene production was observed and color changes from green to red were monitored. Figure 7A shows images of the fruits coated with a layer of PAN@TiO₂ nanofiber and a layer of PP film as well as fruits coated only with a layer of PP film following 14 days of storage at room temperature. Tomatoes coated with PP films turned red, while tomatoes coated with PAN@TiO₂ nanofibers and PP films retained their initial green coloring. The control fruit exhibited rapid ethylene production after 14 days of storage. However, the fruits covered with PAN@TiO₂ nanofibers showed remarkably lower ethylene levels (Figure 7B). The control fruits also exhibited a sharp decrease in firmness, while fruits covered with PAN@TiO₂ nanofibers were much firmer (Figure 7C). Ethylene induces the expression of many ripening-related genes during tomato ripening, such as phytoene synthase (PSY) and polygalacturonase (PG). This leads to lycopene accumulation and cell wall metabolism [27]. Therefore, removal of ethylene from the surrounding atmosphere could delay color change and softening of fruit. These results demonstrate the effectiveness of the PAN@TiO₂ nanofibers in retarding fruit ripening by the degradation of tomato-emitted ethylene.

The implementation of TiO₂ films for the photocatalytic degradation of ethylene in postharvest fruits have been minimally reported. Maneerat and Hayata [10] reported that TiO₂-coated PP film could decompose ethylene in packaged tomatoes under UV light at 1.5 mW cm⁻². Kaewklin et al. [11] employed chitosan and a TiO₂ nanocomposite film to delay tomato ripening by the application of a UV light at an intensity of 42 μW cm⁻². In our study, a low intensity of 2.9 μW cm⁻² was applied for the fruit-ripening test, and the PAN@TiO₂ nanofiber exhibited beneficial effects on extending the

shelf life of tomato fruit. This suggested that the nanofiber was highly efficient for photocatalytic degradation of ethylene and requires little energy. It has been reported that the photocatalytic process also removed acetaldehyde, ethanol, and off-flavors generated by red tomatoes during storage [28]. Although impact on other climacteric fruit is still unclear, and the largescale application still need further investigation, the PAN@TiO₂ nanofiber could be used to remove ethylene from storage and prolong the shelf life of fresh produce.

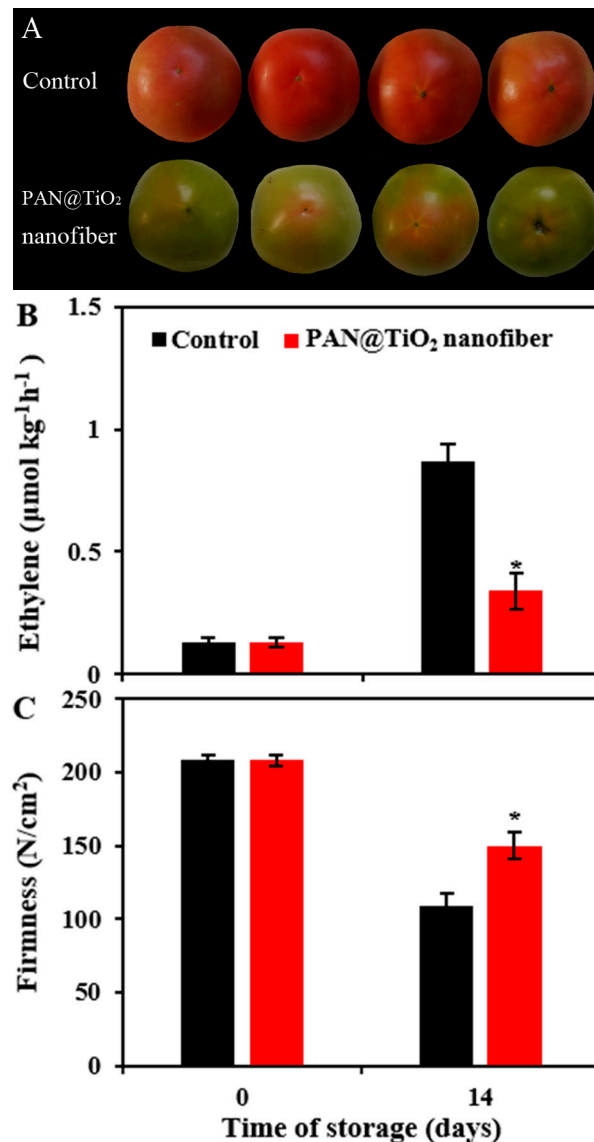


Figure 7. Photographs (a); ethylene production (b); and firmness (c) of tomatoes stored for 14 days covered with PP film (control) or PP film and PAN@TiO₂ nanofibers. The data represent the means of three independent experiments. The error bars indicate the standard deviation of the mean. Asterisks indicate significant differences between the control and nanofiber-covered fruit according to the Student's *t*-test ($P < 0.05$).

4. Conclusions

The present study performed the consecutive electrospinning of PAN and TiO₂ deposition to prepare PAN@TiO₂ nanofibers with uniformly distributed TiO₂ nanoparticles on the nanofiber surface. TiO₂-coated PAN nanofibers showed much higher photocatalytic activity for ethylene degradation than the TiO₂-embedded nanofibers under low-intensity UV light irradiation (2.9 µW cm⁻²). The PAN@TiO₂

nanofibers also exhibited effectiveness in decomposing ethylene emitted by tomatoes and delayed fruit softening and color change during storage at room temperature. Therefore, the PAN@TiO₂ nanofibers has great potential as an ethylene scavenging packaging material for fresh produce during postharvest transportation and storage.

Author Contributions: Z.Z. and Y.W. designed the experimental scheme; Z.Z., Y.Z. (Ye Zhang) and Y.Z. (Yibo Zhang) carried out the measurements; Y.S. and X.Z. performed the theoretical analysis and discussion; Z.Z., Y.Z. (Ye Zhang), Y.Z. (Yibo Zhang) and Y.W. wrote and revised the paper.

Funding: This research was funded by National Key Research and Development Program of China (2018YFD0401302), Beijing Natural Science Foundation (2172039), China Scholarship Council (No. 201806465045), Fundamental Research Funds for the Central Universities and USTB.

Conflicts of Interest: The authors declare no conflict of interest.

References

1. Keller, N.; Ducamp, M.N.; Robert, D.; Keller, V. Ethylene removal and fresh product storage: A challenge at the frontiers of chemistry. Toward an approach by photocatalytic oxidation. *Chem. Rev.* **2013**, *113*, 5029–5070. [[CrossRef](#)] [[PubMed](#)]
2. Tao, G.; Cai, R.; Wang, Y.J.; Song, K.; Guo, P.C.; Zhao, P.; Zuo, H.; He, H.W. Biosynthesis and characterization of AgNPs–Silk/PVA film for potential packaging application. *Materials* **2017**, *10*, 667. [[CrossRef](#)]
3. Wills, R.B.H.; Warton, M.A. Efficacy of potassium permanganate impregnated into alumina beads to reduce atmospheric ethylene. *J. Am. Soc. Hort. Sci.* **2004**, *129*, 433–438. [[CrossRef](#)]
4. Bailén, G.; Guillén, F.; Castillo, S.; Serrano, M.; Valero, D.; Martínez-Romero, D. Use of activated carbon inside modified atmosphere packages to maintain tomato fruit quality during cold storage. *J. Agric. Food Chem.* **2006**, *54*, 2229–2235. [[CrossRef](#)] [[PubMed](#)]
5. Srithamaraj, K.; Magaraphan, R.; Manuspiya, H. Modified porous clay heterostructures by organic-inorganic hybrids for nanocomposite ethylene scavenging/sensor packaging film. *Packag. Technol. Sci.* **2012**, *25*, 63–72. [[CrossRef](#)]
6. Tas, C.E.; Hendessi, S.; Baysal, M.; Unal, S.; Cebeci, F.C.; Menciloglu, Y.Z.; Unal, H. Halloysite nanotubes/polyethylene nanocomposites for active food packaging materials with ethylene scavenging and gas barrier properties. *Food Bioprocess Technol.* **2017**, *10*, 789–798. [[CrossRef](#)]
7. Martínez-Romero, D.; Bailén, G.; Serrano, M.; Guillén, F.; Valverde, J.M.; Zapata, P.; Castillo, S.; Valero, D. Tools to maintain postharvest fruit and vegetable quality through the inhibition of ethylene action: A review. *Crit. Rev. Food Sci.* **2007**, *47*, 543–560. [[CrossRef](#)]
8. Park, D.R.; Zhang, J.; Ikeue, K.; Yamashita, H.; Anpo, M. Photocatalytic oxidation of ethylene to CO₂ and H₂O on ultrafine powdered TiO₂ photocatalysts in the presence of O₂ and H₂O. *J. Catal.* **1999**, *185*, 114–119. [[CrossRef](#)]
9. Tanaka, K.; Fukuyoshi, J.; Segawa, H.; Yoshida, K. Improved photocatalytic activity of zeolite- and silica-incorporated TiO₂ film. *J. Hazard Mater.* **2006**, *137*, 947–951. [[CrossRef](#)]
10. Maneerat, C.; Hayata, Y. Gas-phase photocatalytic oxidation of ethylene with TiO₂-coated packaging film for horticultural products. *Trans. Asabe* **2008**, *51*, 163–168. [[CrossRef](#)]
11. Kaewklin, O.; Siripatrawan, U.; Suwanagul, A.; Lee, Y.S. Active packaging from chitosan-titanium dioxide nanocomposite film for prolonging storage life of tomato fruit. *Int. J. Biol. Macromol.* **2018**, *112*, 523–529. [[CrossRef](#)]
12. Kurtz, I.S.; Schiffman, D.S. Current and emerging approaches to engineer antibacterial and antifouling electrospun nanofibers. *Materials* **2018**, *11*, 1059. [[CrossRef](#)]
13. Zhu, Z.; Zhang, Y.B.; Shang, Y.L.; Wen, Y.Q. Electrospun nanofibers containing TiO₂ for the photocatalytic degradation of ethylene and delaying postharvest ripening of bananas. *Food Bioprocess Technol.* **2019**, *12*, 281–287. [[CrossRef](#)]
14. Hong, Y.L.; Li, D.M.; Zheng, J.; Zou, G.T. In situ growth of ZnO nanocrystals from solid electrospun nanofiber matrixes. *Langmuir* **2006**, *22*, 7331–7334. [[CrossRef](#)]
15. Gupta, K.K.; Mishra, P.K.; Srivastava, P.; Gangwar, M.; Nath, G.; Maiti, P. Hydrothermal in situ preparation of TiO₂ particles onto poly (lactic acid) electrospun nanofibres. *Appl. Surf. Sci.* **2013**, *264*, 375–382. [[CrossRef](#)]

16. Shi, Y.Z.; Yang, D.Z.; Li, Y.; Qu, J.; Yu, Z.Z. Fabrication of PAN@TiO₂/Ag nanofibrous membrane with high visible light response and satisfactory recyclability for dye photocatalytic degradation. *Appl. Surf. Sci.* **2017**, *426*, 622–629. [[CrossRef](#)]
17. Huang, X.S. Fabrication and Properties of Carbon Fibers. *Materials* **2009**, *2*, 2369–2403. [[CrossRef](#)]
18. Zhang, Q.H.; Gao, L.; Guo, J.K. Preparation and characterization of nanosized TiO₂ powders from aqueous TiCl₄ solution. *Nanostruct. Mater.* **1999**, *11*, 1293–1300. [[CrossRef](#)]
19. Kumar, S.G.; Rao, K.S.R.K. Polymorphic phase transition among the titania crystal structures using a solution-based approach: From precursor chemistry to nucleation process. *Nanoscale* **2014**, *6*, 11574–11632. [[CrossRef](#)]
20. Zhang, Y.Y.; Chen, Y.; Hou, L.L.; Guo, F.Y.; Liu, J.C.; Qiu, S.S.; Xu, Y.; Wang, N.; Zhao, Y. Pine-branch-like TiO₂ nanofibrous membrane for high efficiency strong corrosive emulsion separation. *J. Mater. Chem. A* **2017**, *5*, 16134–16138. [[CrossRef](#)]
21. Zhang, J.F.; Zhou, P.; Liu, J.J.; Yu, J.G. New understanding of the difference of photocatalytic activity among anatase, rutile and brookite TiO₂. *Phys. Chem. Chem. Phys.* **2014**, *16*, 20382–20386. [[CrossRef](#)]
22. Xu, N.P.; Shi, Z.F.; Fan, Y.Q.; Dong, J.H.; Shi, J.; Hu, M.Z.C. Effects of particle size of TiO₂ on photocatalytic degradation of methylene blue in aqueous suspensions. *Ind. Eng. Chem. Res.* **1999**, *38*, 373–379. [[CrossRef](#)]
23. Abrams, B.L.; Wilcoxon, J.P. Nanosize semiconductors for photooxidation. *Crit. Rev. Solid Stat.* **2005**, *30*, 153–182. [[CrossRef](#)]
24. Yu, J.G.; Yu, H.G.; Cheng, B.; Zhou, M.H.; Zhao, X.J. Enhanced photocatalytic activity of TiO₂ powder (P25) by hydrothermal treatment. *J. Mol. Catal. A Chem.* **2006**, *253*, 112–118. [[CrossRef](#)]
25. Li, J.; Liu, C.H.; Li, X.; Wang, Z.Q.; Shao, Y.C.; Wang, S.D.; Sun, X.L.; Pong, W.F.; Guo, J.H.; Sham, T.K. Unraveling the origin of visible light capture by core-shell TiO₂. *Chem. Mater.* **2016**, *28*, 4467–4475. [[CrossRef](#)]
26. Tytgat, T.; Hauchecorne, B.; Abakumov, A.M.; Smits, M.; Verbruggen, S.W.; Lenaerts, S. Photocatalytic process optimisation for ethylene oxidation. *Chem. Eng. J.* **2012**, *209*, 494–500. [[CrossRef](#)]
27. Giovannoni, J.J. Fruit ripening mutants yield insights into ripening control. *Curr. Opin. Plant Biol.* **2007**, *10*, 283–289. [[CrossRef](#)]
28. Maneerat, C.; Hayata, Y. Efficiency of TiO₂ photocatalytic reaction on delay of fruit ripening and removal of off-flavors from the fruit storage atmosphere. *Trans. Asabe* **2006**, *49*, 833–837. [[CrossRef](#)]



© 2019 by the authors. Licensee MDPI, Basel, Switzerland. This article is an open access article distributed under the terms and conditions of the Creative Commons Attribution (CC BY) license (<http://creativecommons.org/licenses/by/4.0/>).